This is a repository copy of *A snap-back free Shorted Anode Super-Junction TCIGBT*.

White Rose Research Online URL for this paper:
https://eprints.whiterose.ac.uk/121803/

Version: Accepted Version

Article:

Luo, P., Sweet, M. and Ekkanath Madathil, S. (2018) A snap-back free Shorted Anode Super-Junction TCIGBT. IET Power Electronics, 11 (4). pp. 654-659. ISSN 1755-4535

https://doi.org/10.1049/iet-pel.2017.0407

This paper is a postprint of a paper submitted to and accepted for publication in IET Power Electronics and is subject to Institution of Engineering and Technology Copyright. The copy of record is available at the IET Digital Library

Reuse
Items deposited in White Rose Research Online are protected by copyright, with all rights reserved unless indicated otherwise. They may be downloaded and/or printed for private study, or other acts as permitted by national copyright laws. The publisher or other rights holders may allow further reproduction and re-use of the full text version. This is indicated by the licence information on the White Rose Research Online record for the item.

Takedown
If you consider content in White Rose Research Online to be in breach of UK law, please notify us by emailing eprints@whiterose.ac.uk including the URL of the record and the reason for the withdrawal request.

eprints@whiterose.ac.uk
https://eprints.whiterose.ac.uk/

This article has been accepted for publication in a future issue of this journal, but has not been fully edited.
Content may change prior to final publication in an issue of the journal. To cite the paper please use the doi provided on the Digital Library page.

A snap-back free Shorted Anode Super-Junction TCIGBT

Peng Luo*, Mark R. Sweet, E.M.S. Narayanan

Department of Electronic and Electrical Engineering, The University of Sheffield, Mappin Street, S1 3JD, Sheffield, UK
*pluo2@sheffield.ac.uk

Abstract: A novel structure called the Shorted-Anode Super-Junction Trench Clustered IGBT (SA-SJ-TCIGBT) is proposed and demonstrated through numerical simulations in 1.2-kV, Field-Stop technology. This device is based on the Super-Junction Trench Clustered IGBT (SJ-TCIGBT) concept. In the SA-SJ-TCIGBT structure, due to the introduction of a segmented n^+-anode, the device can operate in both forward conducting mode and freewheeling diode mode without any snap-back in the current voltage characteristics. In comparison to the SJ-TCIGBT structure, the proposed device shows significant improvement in trade-off relationship between forward voltage drop and switch off energy losses. Simulation results show that 25% decrease in switching energy losses can be achieved. Moreover, the tail current is effectively reduced without any increase in the overshoot voltage. Detailed two dimensional modelling of the structure shows that significant amount of excess electrons are extracted through the shorted-anode structure during turn-off process.

1. Introduction

The Insulated gate bipolar transistor (IGBT) is one of the most attractive power semiconductor devices, which is increasingly used in medium power applications, due to its combination of high input impedance and bipolar current conduction. Since the invention of the IGBT, all the IGBT concepts face a trade-off between on-state voltage drop ($V_{ce(sat)}$), turn-off energy losses (E_{off}) and short circuit capability. Hence, the developments of the IGBT are mainly focused upon improving these trade-offs and have almost reached its limits [1]. Moreover, unlike the vertical double-diffusion Power MOSFET which has an intrinsic diode structure [2], the IGBT requires an external anti-parallel Freewheeling Diode (FWD) to protect against reverse conducting currents in various power circuit configurations. Therefore, this will result in additional cost of package and increase Bill of Material (BOM). Recently the Reverse Conducting IGBT (RC-IGBT) concept which can integrate both IGBT and FWD functionalities has drawn a lot of attention [3-5]. It aims to increase power density and improve reliability of the IGBT modules due to reduction of the temperature oscillations [6]. The conventional RC-IGBT structure is similar to the Shorted Anode IGBT (SA-IGBT) structure which employs alternate p-anode and n^+-anode regions at the anode side. Nevertheless, this design suffers from snap-back in the forward I-V characteristics due to the introduction of the n^+-anode which directly connects to the n-buffer region.

Fig. 1 shows a two dimensional cross-section of the RC-TCIGBT while its current voltage characteristics along with a standard TCIGBT are shown in Fig. 2. It can be seen that the conventional TCIGBT shows snap-back free turn-on at 0.7V due to the capacitive coupling between the p-well and p-anode. The RC-TCIGBT can achieve reverse conduction while its forward I-V characteristic exhibits a significant snap-back. It can be explained as follows: during forward conduction, the RC-TCIGBT turns-on when gate voltage is greater than the threshold voltage and anode voltage is positive to the cathode. As depicted in Fig. 1, electrons start to flow through the NMOS channels into the n-drift region and leave the structure via the n+-anode, in the same manner as a unipolar n-channel MOSFET. During this period the current gain is very low due to the absence of conductivity modulation as well as high resistance of the n-drift region. The two-dimensional nature of this electron current flow

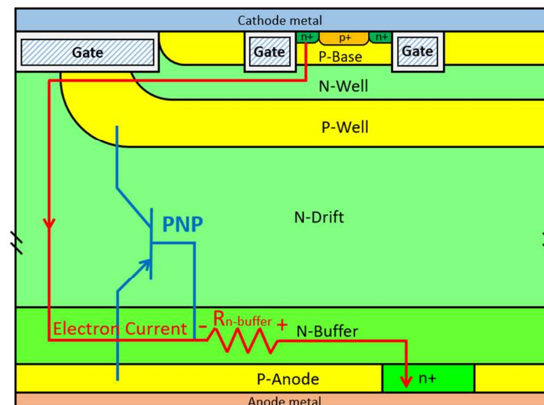

Fig. 1. Simplified cross-section of the RC-TCIGBT.

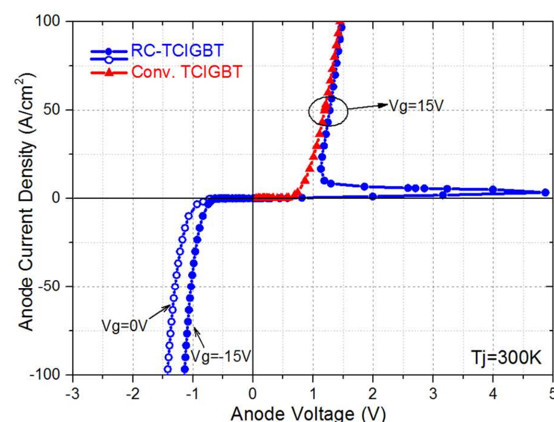

Fig. 2. I-V characteristics of the RC-TCIGBT and the

This article has been accepted for publication in a future issue of this journal, but has not been fully edited.
Content may change prior to final publication in an issue of the journal. To cite the paper please use the doi provided on the Digital Library page.

conventional TCIGBT. τ=10μs.

causes a potential drop across the $R_{n\text{-}buffer}$ which is parallel to the p-anode region. When the potential drop is sufficient to forward bias the p-anode/n-buffer junction, the PNP transistor turns-on and the device operates in the same way as a conventional TCIGBT [7]. The injected charge modulates the conductivity of the n-drift region, decreasing its resistance and causing snap-back in the current voltage characteristic. This snap-back phenomenon has negative influences when the devices are connected in parallel. Consequently, recent developments on RC-IGBTs are focussed upon eliminating this snap-back [8-10]. For example, a novel RC-TCIGBT which combines the conventional CIGBT with an Anti-Parallel Thyristor (APT) was proposed and evaluated in 2007 [8]. The forward IV characteristic shows snap-back free due to the p-anode layer above the n^+-anode acts as a barrier to electrons. Moreover, for the case of reverse conduction, the APT turns-on when the sum of the current gain of each embedded transistor is equal to unity. Another strategy to alleviate snap-back phenomenon was the utilization of deep Super-Junction structure in conventional 3.3-kV IGBT [9]. The on-state resistance during unipolar conduction is significantly reduced by the deep Super-Junction structure. As a result, the forward current density and the potential drop across $R_{n\text{-}buffer}$ are increased at low voltage bias, the snap-back is therefore mitigated.

The Super Junction IGBT concept was introduced in 2002 [11] and further discussions are presented in [12-14]. Recently, the Super Junction Trench Clustered Insulated Gate Bipolar Transistor (SJ-TCIGBT) was proposed and its simulation results have shown significant reduction in both $V_{ce(sat)}$ and E_{off} compared to a standard CIGBT [15]. The improvement of $V_{ce(sat)}$ is contributed by the enhanced conductivity modulation while the reduction of E_{off} is due to the deep p-pillars, which act as the extension of p-well and therefore increase the efficiency of collecting excessive holes within the drift region, during turn-off transient. Furthermore, the issues of turn-off failures as well as poor short circuit capability of conventional SJ-IGBTs are effectively eliminated in the SJ-TCIGBT structure. This is due to: 1) the deep p-pillars connected to the p-well are actually floating and PMOS is introduced for hole currents pass during turn-off process, and 2) the unique self-clamping feature of TCIGBT can clamp n-well potential to a pre-defined value (typically<20V) and therefore help to clean the saturation current density. Thus, the SJ-TCIGBT is a highly promising concept for further development.

In this paper, a novel Shorted Anode Super-Junction Trench CIGBT (SA-SJ-TCIGBT) structure is presented and evaluated through 2-D numerical simulations in the following sections. Compared to the benchmark of SJ-TCIGBT structure, the proposed device introduces an extraction path for excess electrons during turn-off which further improves the $V_{ce(sat)}$-E_{off} trade-offs. Moreover, the SA-SJ-TCIGBT can enable reverse conduction without any snap-back in the I-V characteristics.

2. SA-SJ-TCIGBT Structure and Physics

In order to understand the physics of the proposed SA-SJ-TCIGBT structure, this section firstly explains the fundamental differences between the Trench IGBT (TIGBT) and the TCIGBT. Fig. 3 shows a cross sectional view of comparing the TCIGBT to TIGBT, while Fig. 4 presents the

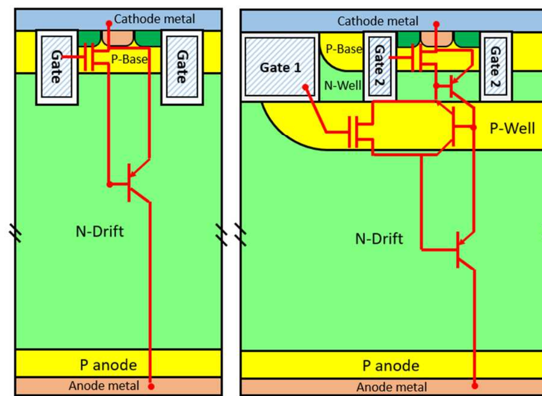

Fig. 3. *Simplified cross-section of the TIGBT and the TCIGBT.*

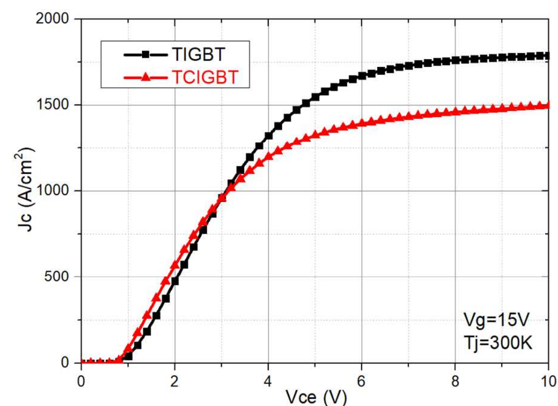

Fig. 4. *I-V characteristics of the TCIGBT and benchmark TIGBT. Main parameters and threshold voltages are kept identical in two structures.*

comparison of I-V characteristics. As shown, compared to the conventional TIGBT which employs a NMOS gate to control a BJT structure, the TCIGBT utilizes a NMOS gate to control a thyristor structure, which comprises of the n-well/p-well/n-drift/p-anode regions. Its turn on mechanism has been explained in [7]. At the cathode side, a number of MOS cells are clustered within a common n-well and p-well layers to form the cathode cells with the main trench Gate-1. All the gates are connected together to make the device a three terminal structure. In order to turn on the device, a positive gate voltage above the MOSFET threshold voltage is applied to form inversion layers in the p-well and p-base regions. Since the inversion layers connect the n-well to the ground potential and the p-well region is floating, the potential in the p-well increases with the anode voltage. Once the potential drop across the p-well/n-well junction is sufficient to forward bias the junction barrier, the main thyristor structure turns on without a snap-back in the forward I-V characteristics. This controlled thyristor action significantly enhances the conductivity modulation within the n-drift region and the linear I-V characteristic is therefore much improved. After the device has been turned on, current is continuously controlled by the MOS gates

This article has been accepted for publication in a future issue of this journal, but has not been fully edited.
Content may change prior to final publication in an issue of the journal. To cite the paper please use the doi provided on the Digital Library page.

Gate-2. As the p-base/n-well junction is reverse biased the depletion boundary within the n-well moves towards the p-well junction as anode voltage increases, this n-well depletion region will punch though at a

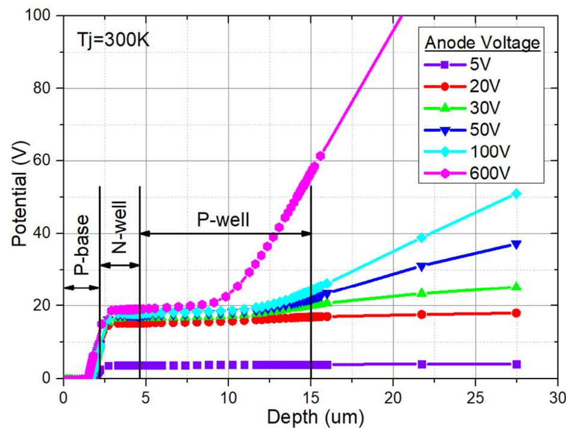

Fig. 5. Simulated potential distributions within TCIGBT structure at various anode voltages. (Vg=15V).

pre-defined voltage, referred to as "self-clamping" voltage. As shown in Fig. 5, any further increase of the anode potential will be supported by the p-well/n-drift junction. Therefore, the cathode cells are protected from exposure to high anode voltages. Most importantly, since the MOS cells are clamped by the self-clamping voltage, the saturation current level is largely independent of forward saturation voltage to achieve wide SOA. This feature is one of the main advantages of TCIGBT over conventional TIGBT technology and its variants.

Fig. 6 and Fig. 7 show the simplified cross-section of the SA-SJ-TCIGBT and its equivalent circuit, respectively. In the SA-SJ-TCIGBT structure, the p channel and n channel MOSFETS (PMOS/NMOS) are connected together to form a common gate electrode, making the device a three terminal device. The PMOS gate is only active during the turn-off cycle when the gate voltage becomes negative with respect to the cathode. Its benefits include: 1) providing p-channels for transporting the excess holes collected by p-well and p-pillars, 2) avoiding the turn-off failure caused by latch-up because a number of holes are flowing into p-channels rather than under the n^+ cathode, 3) connecting the p-base to the p-well and hence enabling reverse conduction as indicated in Fig. 6. At the anode side of the device, a segmented n^+-anode is formed which is carefully controlled so it does not penetrate the p-anode region. The advantages of this design are to provide a direct extraction path for excessive electrons during turn-off process and to act as the n^+ cathode of the FWD during reverse conduction. In addition, compared to the conventional RC-TCIGBT, the proposed shorted-anode structure can enable the device to realize snap-back free turn-on in the I-V characteristics.

During forward conduction, the operation principle of the SA-SJ-TCIGBT is as same as that of a standard TCIGBT. The device turns-on when the gate voltage is greater than the NMOS threshold voltage and the anode voltage is greater than 0.7V. In the reverse conduction, the gate voltage pulse is changed from +15 V to -15 V. Thus, the NMOS gates turn-off whereas the PMOS gate turns-on. Additionally, the p-base and the p-well are connected by the p-channels, as highlighted in Fig. 6. At the cathode side of the FWD, as shown in Fig. 10, there exists a base-emitter shorted NPN transistor, T_{npn1},

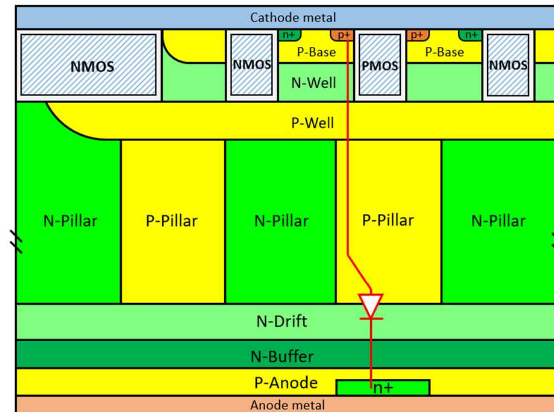

Fig. 6. Simplified cross-section of the proposed SA-SJ-TCIGBT.

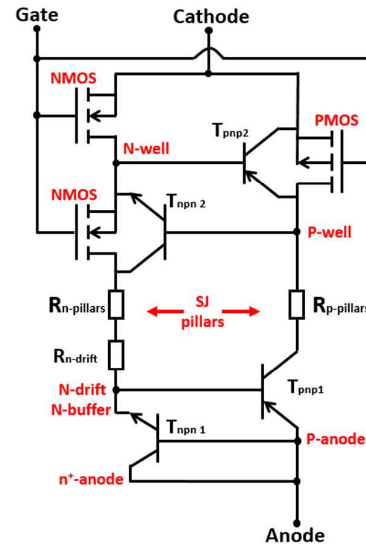

Fig. 7. Equivalent circuit of the SA-SJ-TCIGBT.

consisting of n-buffer, p-anode and n^+-anode. The doping concentration and dimensions of the n^+-anode are carefully controlled to ensure that the base of T_{npn1} is easily punched through when the FWD turns-on. A specific demonstration of this process is given in next section.

3. Simulation Results and Analysis

3.1. Blocking Performance

Fig. 8(a) shows the depletion boundaries within SA-SJ-TCIGBT structure under forward blocking state at 1.2 kV, while Fig. 8(b) shows the simulated electric field profiles across n-pillars and p-pillars, respectively. In the SA-SJ-TCIGBT device, the charge Q in n-pillars and p-pillars are exactly balanced in order to enable the SJ structure to block maximum voltage. Under static blocking condition, the

This article has been accepted for publication in a future issue of this journal, but has not been fully edited.
Content may change prior to final publication in an issue of the journal. To cite the paper please use the doi provided on the Digital Library page.

narrow n-well layer is completely depleted. Therefore, the blocking voltage is mainly supported by SJ structure as well as n-drift region.

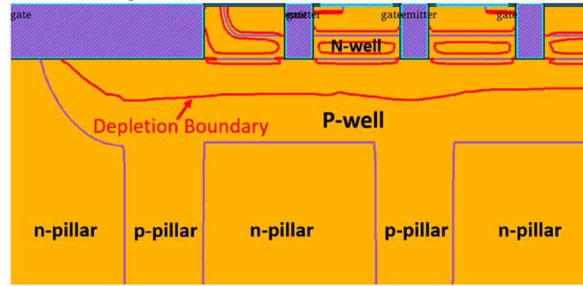

(a)

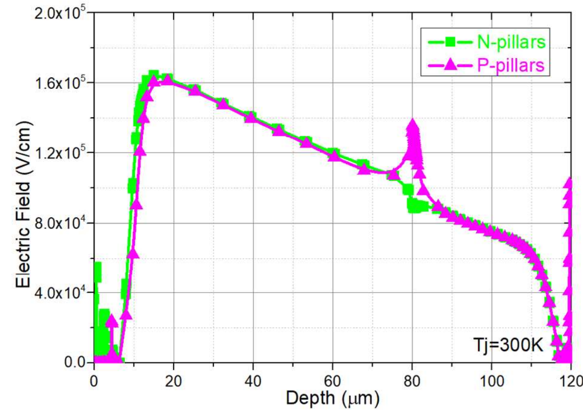

(b)

Fig. 8. ***(a)*** *Simulated depletion boundaries within SA-SJ-TCIGBT under forward blocking state. (Vanode=1200 V)* ***(b)*** *1-D electric field distributions across n-pillars and p-pillars respectively.*

3.2. On-State Performance

In order to compare the electrical performances, the parameters of the SA-SJ-TCIGBT are identical to that of the benchmark SJ-TCIGBT, except for the additional segmented n^+-anode region. Fig. 9 shows the I-V characteristics of the proposed SA-SJ-TCIGBT at T_j = 300 K. During forward conduction, due to the n^+-anode and the p-anode are shorted, and the p-anode layer above the n^+-anode provides a sufficient barrier to prevent electrons from entering the anode prior to turn-on of the main thyristor, the device therefore shows snap-back free turn-on and operates successfully as the conventional SJ-TCIGBT. However, the $V_{ce(sat)}$ of the SA-SJ-TCIGBT, measured at a current density of 100 A/cm^2, is 1.49V, which is 6% greater than that of the comparative SJ-TCIGBT structure of 1.41 V. This can be attributed to a slight reduction of p-anode area which reduces the anode injection. Furthermore, during reverse conduction, the FWD turns-on at approximately 0.7 V without snap-back. This can be explained as the base region of the T_{npn1} is punched though when V_{anode} = -0.7 V. Fig. 11 depicts the electric field and potential distribution through the cut line A-A' shown in Fig. 10 at anode voltages of 0 V and -0.7 V, respectively. As shown, the electric field and potential are almost constant through the n-buffer/p-anode junction and the majority of the p-anode region when the anode voltage is -0.7 V. In addition, both the electric field at the p-anode/n^+-anode junction and the potential drop across this junction significantly decreases when compared to the OFF state, V_{anode} = 0 V. Consequently,

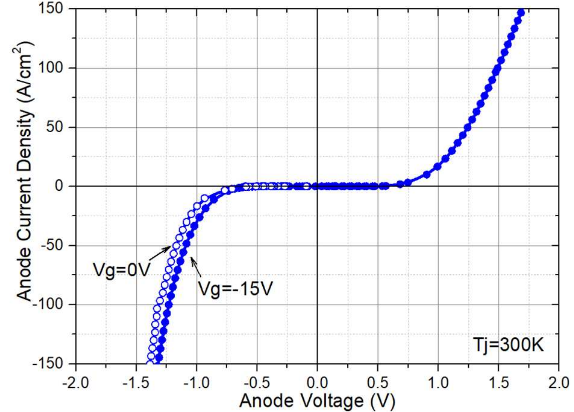

Fig. 9. *I-V characteristics of the SA-SJ-TCIGBT. (n:p width ratio=20% : 80%, τ=10μs, T_j= 300 K)*

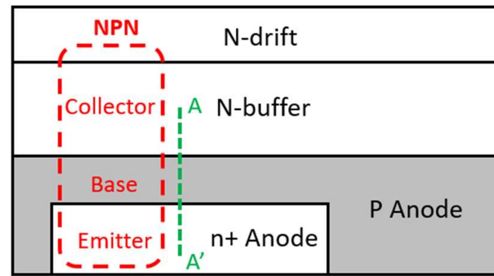

Fig. 10. *The equivalent NPN transistor structure at the cathode side of the FWD.*

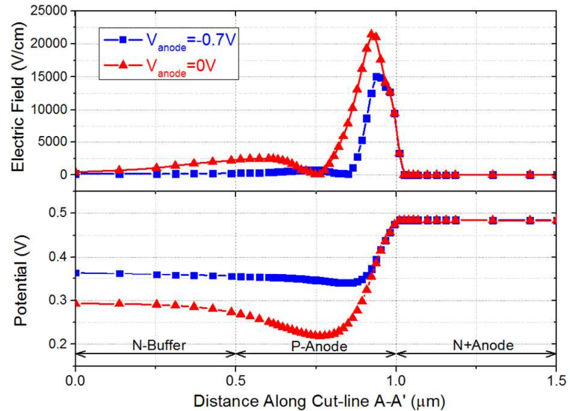

Fig. 11. *Electric fields and potentials across the shorted anode structure. (V_g=-15V, T_j=300K, τ=10μs, cathode is grounded)*

it can be verified that the p-anode layer has been depleted when V_{anode} = -0.7 V. Under this condition, the n-buffer and the n^+-anode are connected together and electrons are injected into the drift region via the n^+-anode contact. The device works like a conventional PiN diode.

3.3. Inductive Switching Performance

IET Review Copy Only

This article has been accepted for publication in a future issue of this journal, but has not been fully edited.
Content may change prior to final publication in an issue of the journal. To cite the paper please use the doi provided on the Digital Library page.

Fig. 12 shows the inductive switching test circuit used in the simulations, while Fig. 13 shows the inductive turn-off waveforms of the SA-SJ-TCIGBT with respect to the SJ-TCIGBT structure. These characteristics are taken when the

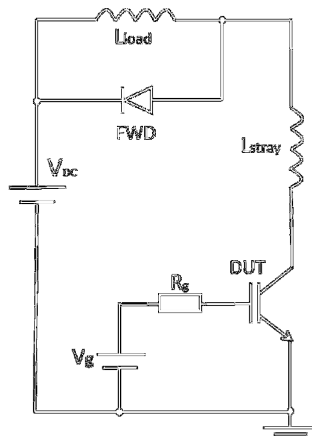

Fig. 12. *Inductive switching test circuit. (V_{DC}=600V, V_g=±15V, L_{stray}=100nH, and R_g=5Ω)*

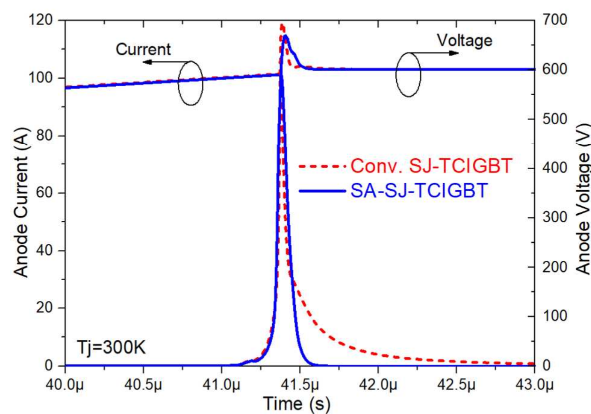

Fig. 13*. Turn-off waveforms of the SJ-TCIGBT and the SA-SJ-TCIGBT. (n:p width ratio=20% : 80%, τ=10μs)*

device turns-off 100 A at 100 A/cm^2 and an applied anode voltage of 600V. Parasitic anode inductance of 100 nH has been considered for these mixed mode transient simulations. During the turn-off transient of the conventional SJ-TCIGBT, due to the existence of an open base PNP transistor, consisting of p-pillars, n-drift/n-buffer and p-anode, the excessive electrons within the drift region must recombine with holes and there are no external means to sweep them out. Moreover, the electrons flowing into the p-anode region will result in a back injection of holes into the drift region and therefore slow down the turn-off speed. In contrast, for the case of SA-SJ-TCIGBT structure, the segmented n$^+$-anode structure can effectively extract the stored electrons. As a result, as shown in Fig. 13, the SA-SJ-TCIGBT exhibits a significant reduction in current tail without any increase in overshoot voltage compared to that of the conventional SJ-TCIGBT. Fig. 14(a) depicts the current flow lines through the shorted-anode structure during tail current phase. Due to the great barrier height of the p-anode/n$^+$-anode junction, the current flowing into the shorted-anode structure is mainly contributed by electron current. Any electron flowing into the T_{npn1} will be swept out by the electric field formed by the built-in potential of p-anode/n$^+$-anode junction. Therefore, it is clearly evident that a significant proportion of electrons evacuate through the segmented p-anode and enter the n$^+$-

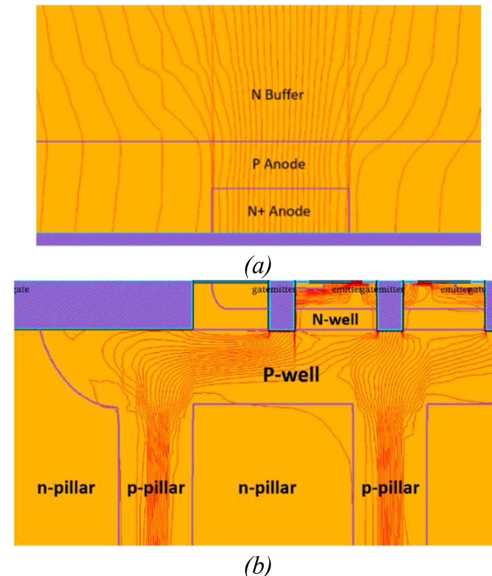

Fig. 14. *Current flow lines during tail current phase with V_g=-15V.* ***(a)*** *anode side.* ***(b)*** *cathode side.*

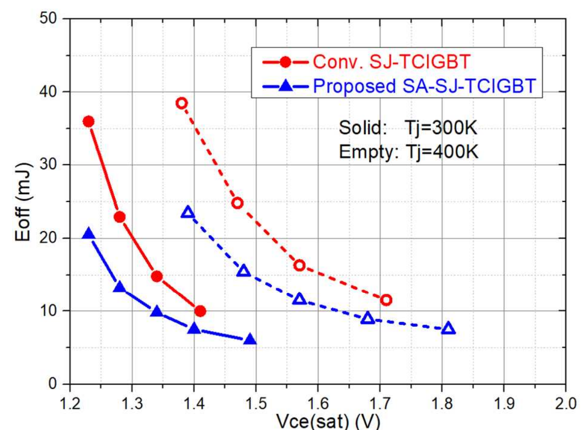

Fig. 15*. The $V_{ce(sat)}$-E_{off} trade-offs of SA-SJTCIGBT and benchmark. (n:p width ratio=20% : 80%, τ=10μs)*

anode region during turn-off phase. Since excess electrons are effectively removed from the drift region, the E_{off} of the SA-SJ-TCIGBT is much lower in comparison to the E_{off} of the conventional SJ-TCIGBT. Moreover, Fig. 14(b) clearly shows that the excess holes in the drift region are collected by the p-pillars and flow through the p-well then into the PMOS channels. Hence, in the SA-SJ-TCIGBT structure, both excess electrons and holes are effectively removed through the evacuation paths at the anode side and cathode side, respectively.

Fig. 15 shows the $Vce_{(sat)}$-E_{off} trade-offs of the proposed SA-SJ-TCIGBT compared to the conventional SJ-TCIGBT. The trade-off curves are obtained when modifying

This article has been accepted for publication in a future issue of this journal, but has not been fully edited.
Content may change prior to final publication in an issue of the journal. To cite the paper please use the doi provided on the Digital Library page.

the p-anode peak doping concentration from 5e17 cm^{-3} to 1e19 cm^{-3}. As shown, due to the enhanced carrier removal, for an identical forward voltage drop, the SA-SJ-TCIGBT exhibits at least 25% reduction in switching energy losses at both T_j = 300 K and T_j = 400 K. Therefore, the proposed SA-SJ-TCIGBT can achieve superior switching speed while still maintain low forward voltage drop.

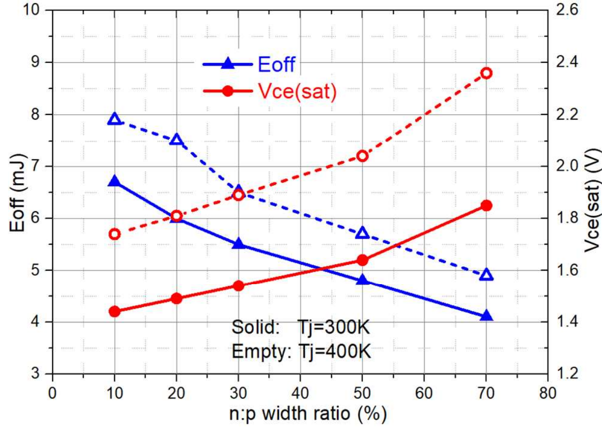

***Fig. 16.** Influence of n: p width ratio on $V_{ce(sat)}$-E_{off} trade-offs. (τ =10μs)*

3.4. Influence of n: p Width Ratio

The influence of the width ratio of the n^+-anode and p-anode upon forward voltage drop as well as switching energy losses is shown in Fig. 16. As shown, as the n: p width ratio increases, the forward voltage drop increases due to the reduced anode injection. However, this also causes the switching energy losses reduce due to a smaller level of conductivity modulation.

3.5. Influence of Pillars Depth

Since all the excess holes stored within the drift region are mainly transported by p-pillars and p-well region, therefore, the depth of the pillars has an influence on the turn-off energy losses. Fig. 17 shows the influence of pillars depth on the $V_{ce(sat)}$-E_{off} trade-off. It can be seen that E_{off} decreases with deep pillars due to reduced tail current, while the $V_{ce(sat)}$ is only slightly affected due to the thyristor conduction enables the on-state carrier's concentration is at least one order of magnitude higher than the pillars doping concentration, as shown in Fig. 18.

4. Conclusion

The electrical performances of the proposed SA-SJ-TCIGBT compared with the conventional SJ-TCIGBT have been evaluated with mixed mode two dimensional TCAD simulations. Detailed simulation results show that the SA-SJ-TCIGBT can operate in both forward and reverse conducting mode without any snap-back in the current-voltage characteristics. In addition, the shorted anode structure proposed in this paper can reduce the switching energy losses effectively due to improved charge removal as a result of the segmented n^+-anode structure. From fabrication point of view, the SA-SJ-TCIGBT structure requires only one additional photolithographic masking step and temperature cycle compared to the SJ-TCIGBT processes discussed in [15]. The dose and depth of the segmented n^+-anode have to be exactly controlled. Although additional fabrication cost is required, both the $V_{ce(sat)}$-E_{off} trade-off and the power density of the modules can be significantly improved.

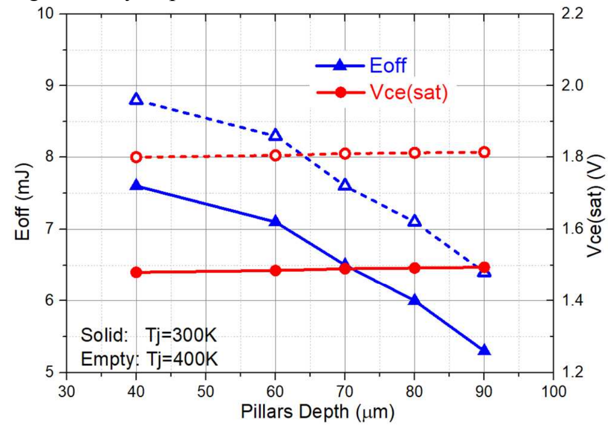

***Fig. 17.** Influence of pillars depth on $V_{ce(sat)}$-E_{off} trade-offs. (τ =10μs)*

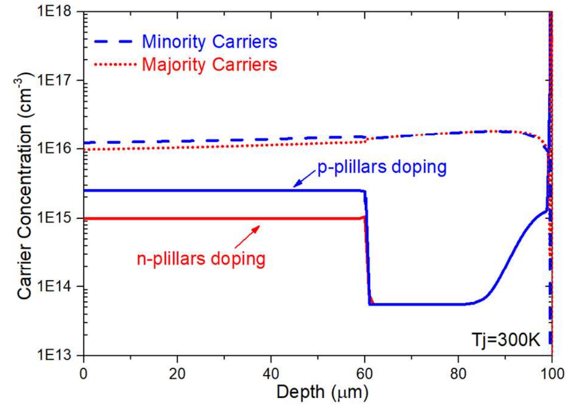

***Fig. 18.** Comparison between Super-Junction doping concentration and on-state carrier's distribution at a current density of 100A/cm^{-2}. (τ =10μs)*

5. References

[1] A. Huang, "Recent advances and applications of power electronics and motor drives - Power semiconductor devices," presented at the 2008 34th Annual Conference of IEEE Industrial Electronics, 2008.

[2] T. Minato, S. Aono, K. Uryu, and T. Yamaguchi, "Making a bridge from SJ-MOSFET to IGBT via RC-IGBT structure Concept for 600V class SJ-RC-IGBT in a single chip solution," in *2012 24th International Symposium on Power Semiconductor Devices and ICs*, 2012, pp. 137-140.

[3] Takahashi, Yamamoto, Aono, and Minato, "1200V reverse conducting IGBT," in *2004 Proceedings of the 16th International Symposium on Power Semiconductor Devices and ICs*, 2004, pp. 133-136.

[4] T. Yoshida, T. Takahashi, K. Suzuki, and M. Tarutani, "The second-generation 600V RC-IGBT with optimized FWD," in *2016 28th International Symposium on Power Semiconductor Devices and ICs (ISPSD)*, 2016, pp. 159-162.

This article has been accepted for publication in a future issue of this journal, but has not been fully edited.
Content may change prior to final publication in an issue of the journal. To cite the paper please use the doi provided on the Digital Library page.

[5] M. Rahimo, A. Kopta, U. Schlapbach, J. Vobecky, R. Schnell, and S. Klaka, "The Bi-mode Insulated Gate Transistor (BIGT) a potential technology for higher power applications," in *2009 21st International Symposium on Power Semiconductor Devices & IC's*, 2009, pp. 283-286.

[6] L. Storasta, A. Kopta, and M. Rahimo, "A comparison of charge dynamics in the reverse-conducting RC IGBT and Bi-mode Insulated Gate Transistor BiGT," in *2010 22nd International Symposium on Power Semiconductor Devices & IC's (ISPSD)*, 2010, pp. 391-394.

[7] O. Spulber, M. Sweet, K. Vershinin, C. K. Ngw, L. Ngwendson, J. V. S. C. Bose*, et al.*, "A novel trench clustered insulated gate bipolar transistor (TCIGBT)," *IEEE Electron Device Letters,* vol. 21, pp. 613-615, 2000.

[8] D. Kumar, M. Sweet, K. Vershinin, L. Ngwendson, and E. M. S. Narayanan, "RC-TCIGBT: A Reverse Conducting Trench Clustered," in *Proceedings of the 19th International Symposium on Power Semiconductor Devices and IC's*, 2007, pp. 161-164.

[9] M. Antoniou, F. Udrea, F. Bauer, and I. Nistor, "A new way to alleviate the RC IGBT snapback phenomenon: The Super Junction solution," in *2010 22nd International Symposium on Power Semiconductor Devices & IC's (ISPSD)*, 2010, pp. 153-156.

[10] W. C. W. Hsu, F. Udrea, H. Y. Hsu, and W. C. Lin, "Reverse-conducting insulated gate bipolar transistor with an anti-parallel thyristor," in *2010 22nd International Symposium on Power Semiconductor Devices & IC's (ISPSD)*, 2010, pp. 149-152.

[11] F. Bauer, "The MOS controlled super junction transistor (SJBT): a new, highly efficient, high power semiconductor device for medium to high voltage applications," in *Proceedings of the 14th International Symposium on Power Semiconductor Devices and Ics*, 2002, pp. 197-200.

[12] M. Antoniou, F. Udrea, and F. Bauer, "The Superjunction Insulated Gate Bipolar Transistor Optimization and Modeling," *IEEE Transactions on Electron Devices,* vol. 57, pp. 594-600, 2010.

[13] F. Bauer, I. Nistor, A. Mihaila, M. Antoniou, and F. Udrea, "SuperJunction IGBTS: An evolutionary step of silicon power devices with high impact potential," in *CAS 2012 (International Semiconductor Conference)*, 2012, pp. 27-36.

[14] F. Bauer, I. Nistor, A. Mihaila, M. Antoniou, and F. Udrea, "Superjunction IGBT Filling the Gap Between SJ MOSFET and Ultrafast IGBT," *IEEE Electron Device Letters,* vol. 33, pp. 1288-1290, 2012.

[15] N. Luther-King, M. Sweet, and E. M. S. Narayanan, "Clustered Insulated Gate Bipolar Transistor in the Super Junction Concept: The SJ-TCIGBT," *IEEE Transactions on Power Electronics,* vol. 27, pp. 3072-3080, 2012.